Colloids and Surfaces B: Biointerfaces 165 (2018) 18–27

Contents lists available at ScienceDirect

Colloids and Surfaces B: Biointerfaces

journal homepage: www.elsevier.com/locate/colsurfb

Development of an indolicidin-derived peptide by reducing membrane perturbation to decrease cytotoxicity and maintain gene delivery ability

Ching-Wei Tsai [a], Ze-Wei Lin [a], Wen-Fang Chang [a], Yi-Fan Chen [a], Wei-Wen Hu [a,b,*]

[a] Department of Chemical and Materials Engineering, National Central University, No. 300, Jhongda Rd., Jhongli District, Taoyuan City, 32001, Taiwan
[b] Center for Biocellular Engineering, National Central University, No. 300, Jhongda Rd., Jhongli District, Taoyuan City, 32001, Taiwan

ARTICLE INFO

Article history:
Received 27 October 2017
Received in revised form 30 January 2018
Accepted 3 February 2018
Available online 5 February 2018

Keywords:
Indolicidin
Cell penetrating peptides (CPPs)
Membrane perturbation
Gene delivery
Cytotoxicity
Molecular dynamics (MD) simulation

ABSTRACT

Indolicidin (IL) is a cationic antimicrobial peptide and our previous study has demonstrated its potential as a cell penetrating peptide (CPP) to promote gene delivery. However, the cytotoxicity of IL arisen from its membrane perturbation capacity may restrict its clinical application. To promote gene delivery safety and efficiency, an almost mirror-symmetric IL derivative, SAP10 (RRWKFFPWRR-$CONH_2$), was designed in this study. All-atom molecular dynamics (MD) simulations were performed to understand the association between SAP10 and model lipid bilayers. By comparison with IL, SAP10 with high positively charged density resisted its deep insertion into lipid bilayers, which thus reduced its perturbation to lipid bilayers and improved biocompatibility. Consequently, we further mixed SAP10, polyethylenimine (PEI) and DNA to form the ternary nanocomplexes for gene delivery investigation. Both IL and SAP10 weakened the interaction between to DNA and PEI, which may be beneficial to promote the dissociation of internalized DNA from the carrier molecules. *In vitro* experiments demonstrated that the SAP10-associated ternary nanocomplexes highly promoted the transfection efficiency to various cells with low cytotoxicity. The effect of the SAP10 on promoting gene delivery was mainly contributed by the adsorbed peptides on the nanoparticles rather than the free ones. In particular, the dose of SAP10 could be increased to broaden the administration window, which ensured its safety on transfection. Therefore, our results suggested the argument that the designed SAP10 is a safe and an efficient peptide to promote PEI-mediated gene delivery.

© 2018 Elsevier B.V. All rights reserved.

1. Introduction

For gene delivery, an appropriate carrier is extremely important because anionic nucleic acid cannot directly penetrate cell membrane. To overcome the cell membrane barrier, cell-penetrating peptides (CPPs) is considered as potential carriers because of their membrane penetration capability [1,2]. Depending on their structures, there are several models to explain the translocation mechanism of CPPs. For example, amphipathic peptides, such as transportan, may insert into the membrane and adopt α-helical conformation to induce pore formation [3]. Cationic peptides, such as penetratin, have strong electrostatic interaction with phospholipids to induce their translocation to the hydrophobic cavity of lipid bilayer and form inverted micelles, which then is released in the reverse process [4]. Arginine-rich peptides, such as TAT, their guanidinium groups can interact with anionic phospholipids to form lipophilic ion pairs, which can diffuse along the membrane potential inside the cells [5]. Therefore, the transport of CPPs is mono-directional that the internalized contents can remain inside the cell [6,7]. Although the delivery mechanism of CPPs is still under debate, their translocation obviously relative to the perturbation of cell membrane, which probably elicits potential cytotoxicity [8–10].

Indolicidin (IL) is a well-known cationic antimicrobial peptide derived from bovine neutrophils. Because IL is rich in cationic arginine/lysine and hydrophobic tryptophan (ILPWKWPWWPWRR-$CONH_2$), it can interact to anionic cellular membrane and exhibit as an extended structure in lipid bilayer [11]. Indolicidin has been broadly applied as an alternative of antibiotics due to its perturbation which eventually causes membrane disruption [12]. Its Trp 8 & Trp 9 in the *C*-terminal domain have been proved to

* Corresponding author at: Department of Chemical and Materials Engineering, National Central University, No. 300, Jhongda Rd., Jhongli District, Taoyuan City, 32001, Taiwan.
E-mail address: huweiwen@cc.ncu.edu.tw (W.-W. Hu).

https://doi.org/10.1016/j.colsurfb.2018.02.007
0927-7765/© 2018 Elsevier B.V. All rights reserved.

perturb head-groups and hydrophobic core of mammalian-mimic membrane significantly [13]. Such membrane penetration ability implies that IL is potential to carry cargo as CPPs [14]. Therefore, we have demonstrated that IL can be an adjuvant to facilitate polyethylenimine (PEI)-mediated gene delivery [15]. Although the transfection efficiency was highly improved, we also found that the cytotoxicity of IL limits its application. Similar toxicity of IL has also been reported to its treatment to erythrocytes and T lymphocytes [11,16]. The hemolytic activity is likely elicited by the aggregation of IL in aqueous environment [17]. As IL inserts to hydrophobic environment, such as the interior cavity of lipid bilayer, the aggregation is greatly promoted which thus destroys membrane structure. In addition, the membrane leakage induced by amphipathic peptides seems to correlate with their hydrophobic moments [18]. The cytotoxicity of IL also has been proved to be relative to its hydrophobic tryptophan residues [19]. These results all indicated that decreasing hydrophobicity of IL should be able to reduce it membrane perturbation and cytotoxicity.

In our previous study, we have designed an IL derivative, IL-K7F89 (ILPWKWKFFPWRR-$CONH_2$). Compared to the IL, IL-K7F89 is a potential IL analogue with not only low hemolytic activity but also high antibacterial capability [13]. These results reveal that the amino acids changed in the C-terminal domain of IL may significantly reduce its disruption of erythrocytes. Therefore, we developed a mirror-symmetric peptide, SAP10, which was derived from C-terminal of IL and replaced partial of tryptophan by phenylalanine. Both molecular dynamics (MD) simulation and small-angle X-ray scattering (SAXS) analysis were performed to investigate the interaction between SAP10 and lipid bilayer. For gene delivery application, IL or SAP10 peptides were mixed with DNA and PEI to form ternary particles, and their transfection efficiency as well as biocompatibility were compared to determine whether the modified SAP10 peptide can reduce cytotoxicity and maintain transfection capability.

2. Experimental section

2.1. Materials

The indolicidin (ILPWKWPWWPWRR-$CONH_2$), SAP10 (RRWKFFPWRR-$CONH_2$), and R9 (RRRRRRRRR-$CONH_2$) peptides were obtained from MDBio, Inc. (Taipei, Taiwan) with purity higher than 95%. Tetradecane, 2-methylbutane, ethidium bromide (EtBr), 5-bromo-4-chloro-3-indolyl-b-D-galactopyranoside (X-gal), ortho-nitrophenyl-β-D-galactopyranoside (ONPG), 4′,6-diamidino-2-phenylindole (DAPI), alginate with molecular weight of 80–100 kDa, and polyethylenimine (PEI) with molecular weight of 750 kDa were purchased from Sigma-Aldrich (St. Louis, MO, USA). N,N-dimethyl formamide (DMF) was bought from Acros (Geel, Belgium). Dioleoylphosphatidylethanolamine (DOPE) dissolved in chloroform was obtained from Avanti (Alabaster, AL, USA); the DOPE stock solution was stored at −20 °C before the sample preparation.

2.2. Membrane perturbation by molecular dynamics (MD) simulation

All-atom MD simulations were applied to study the membrane perturbation of peptides. IL and SAP10 peptides were inputted into the MD simulations in the presence of zwitterionic 1-palmitoyl-2-oleoyl-sn-glycero-3-phosphocholine (POPC) lipid bilayers which were used to mimic the membrane of erythrocytes [20]. The modeling systems contain a peptide, 98 lipids (49 lipids for each leaflet), 5834 waters, and the counterions Na^+ and Cl^- were added to neutralize the system and yielded a salt concentration of 0.15 M for each system. Because both IL and SAP10 exhibited random in phosphate buffered saline (PBS) environment, these two peptides with extended structure were put 5 Å above the surface of membrane bilayers [21]. All initial configurations of these systems were constructed using the VMD program and the CHARMM-GUI [22]. MD simulations were performed using the CHARMM36 all-atom force field [23] with the backbone phi/psi dihedral angle cross-term correction [24]. The water molecules were simulated using the TIP3 model [25]. MD simulations were run with an NPT ensemble at 310 K and 1 bar under three-dimensional periodic boundary conditions by parallel MD NAMD 2.7b3 software [26]. Long-range electrostatic interactions were determined by the particle-mesh Ewald technique. Cutoffs at 12.0 and 13.5 Å were applied to calculate the pair-wise interactions and generate the neighboring list of pairs, respectively. The non-bonded neighboring list was updated every 10 time steps. The force switching function was applied to smooth the non-bonded electrostatics and van der Waals potential energy whenever the internuclear distance of two atoms was between 9 and 12.0 Å [27]. An integration time step of 2 fs was used by constraining the hydrogen atom-involved covalent bond lengths via the SHAKE algorithm [28]. Before performing the production simulations, each system was minimized using a conjugate gradient algorithm to avoid bad contacts of the initial configuration. After 100,000 minimization steps, an energy tolerance of 0.0001 kcal/mol was reached for each modeling system. Then a 0.1-ns slow heating simulation was performed until the system temperature achieved 310 K. In addition, the trajectories were recorded every 5 ps. MD simulations were performed for each system for a 80 ns duration and the last 20 ns trajectory was used for statistical analysis.

The order parameters of peptide-membrane interaction were calculated to measure of the ordering of lipid molecules. It indicated possible structural deformations/perturbation of a lipid bilayer. The order parameter of the membrane's acyl chains was defined by the function $< S_{CC} >= \frac{1}{2}\langle 3\cos^2(\theta_i) - 1\rangle$, where θ_i was the angle between the directions of the carbon atom of the acyl SN1 chain at positions i and i–1 and the membrane normal. The symbol <> denoted the average over time.

2.3. Hemolysis analysis

Hemolytic activity of peptides was evaluated through measuring the release of hemoglobin from human red blood cells (RBCs). These RBCs were separated by centrifuging whole blood collected from a healthy donor at 3000 rpm for 10 min at 4 °C. Through removing the supernatant and washed by PBS, 1% (v/v) of RBCs in PBS was gently mixed with peptide in concentrations of 0–64 μM. After incubating at 37 °C for 1 h, the samples were centrifuged for 5 min at 1000 rpm, and their supernatants were analyzed spectrophotometrically at a wavelength of 540 nm (Synergy H1m, Biotek, Winooski, VT, USA). The absorbance results by mixing RBCs with PBS only and PBS with 1 wt% Triton-X100 were defined as 0 and 100% hemolysis, respectively.

2.4. Small-angle X-ray scattering (SAXS)

To prepare the SAXS sample, DOPE films were used to mimic the mammalian cells [29]. A specific amount of the DOPE stock solution with the DOPE dry weight of 8 mg was dispensed into a Teflon-capped glass vial. Chloroform was evaporated by a gentle flow of argon gas, followed by an overnight incubation in vacuum. The obtained dry film of DOPE was mixed with tetradecane in 2-methylbutane under vigorous vortex to relieve the packing frustration of the lipid hydrocarbon chains and thereby make the spontaneous curvature measurable [30]. 2-methylbutane was evaporated following the same procedures as for removing chloroform; the concentration of tetradecane in the dry film of

DOPE-tetradecane was fixed at 16 wt%. The dry film was subsequently resuspended in the excessive 10 mM PBS buffer (pH = 7.4) containing 800 μM IL or SAP10. The suspension was pressed alternately between two glass syringes equipped with stainless steel plungers for approximately 100 times, followed by 10 freeze-thaw cycles to homogenize the sample.

The X-ray experiments were conducted with the CuK_α radiation generated from an X-ray generator (NANO-Viewer, Rigaku, Japan) and with the synchrotron radiation at Beamlines BL13A1 and BL23A1 of the National Synchrotron Radiation Research Center in Hsinchu, Taiwan [31]. The X-ray generator was operated at 40 kV and 30 mA, while 12 keV and 15 keV X-rays at BL13A1 and BL23A1, respectively, were used for the X-ray experiments. The X-ray data were collected with a 2D pixel detector (PILATUS 100 K, Dectris, Switzerland) for the X-ray generator, and with a Mar165 CCD detector and PILATUS 1MF pixel detector at BL13A1 and BL23A1, respectively. The collected data were reduced, azimuthally integrated and used for the reconstruction of the electron density profile following the steps detailed in Chen et al. [30] to determine the value of the monolayer spontaneous curvature.

2.5. Plasmid DNA preparation

The reporter gene β-galactosidase encoded plasmid pCMV-β was purchased from Clontech (Mountain View, CA, USA). Competent cells *Escherichia Coli* DH5α (Invitrogen, Carlsbad, CA, USA) was used to clone and amplify pCMV-β. The harvested plasmid DNA was purified by sodium hydroxide isolation and phenol/chloroform extraction. The purified plasmid DNA was qualified by the PCR detection, restriction enzyme mapping, and DNA sequencing analysis.

2.6. Preparation of DNA/peptide/PEI ternary complexes

The construction proportions of nanoparticles were expressed as the ratios of amino groups of carrier molecules to phosphate groups of DNA (N/P ratios). DNA concentration was fixed to 20 ng/μl and the N/P ratio of PEI to DNA was maintained to 10. All materials were dissolved in phosphate buffer saline (PBS). Initially, 12.5 μL of peptide was added to 12.5 μL of DNA before mixing by vortex. After 30 min incubation at room temperature, 25 μL of PEI was slowly added to the mixture drop by drop. The prepared nanoparticles were incubated for 30 min before transfection.

2.7. Characterization of gene transfer vectors

Dynamic light scattering (DLS) analysis was applied to determine the zeta potentials and sizes of nanoparticles using Zetasizer Nano ZS (Nalvern, Worcestershire, UK). Samples with volume of 0.8 mL were loaded in disposable capillary cells, and the electrophoretic mobilities of nanoparticles were measured to calculate their zeta potentials. Furthermore, photon correlation spectroscopy at a 173° scattering angle was used to determine size distribution. Three measurements were performed per sample, and the mean hydrodynamic diameter was calculated by cumulative analysis.

2.8. The complexation efficiency

The loading capacity of peptide/PEI to DNA was analyzed by gel retardation and EtBr displacement assays. About gel retardation assay, nanocomplexes were loaded in 1 wt.% agarose gels to perform electrophoresis for 40 min at 100 V and were stained by EtBr. For the EtBr displacement assay, DNA was mixed with EtBr (DNA base: EtBr (mol) = 200:1) before complexing with peptide and PEI. These samples were incubated at room temperature for 30 min, and then 100 μL of each was transferred to 96-well microplates and measured by fluorescence spectrometry (Synergy H1m, Biotek, Winooski, VT, USA) with an excitation wavelength at 511 nm and emission wavelength at 603 nm. The results were compared to the read of DNA without complexation to determine the relative EtBr displacement.

2.9. Competition assay for comparing the interaction between carrier and DNA

To determine the affinity between DNA and carriers, anionic alginate was applied to compete with DNA. After mixing EtBr with DNA (DNA base: EtBr (mol) = 200:1), peptides and PEI were added sequentially to fabricate ternary nanoparticles. Equal volume of alginate in PBS (0.42 g/l) was then added to these complexs, and the untreated groups were those added PBS instead of alginate solution. After 20 min incubation, the nanoparticles with or without alginate treatment were analyzed by fluorescence spectrometry, and the relative EtBr displacement was determined by comparing to the read of DNA without complexation. The reduction of EtBr displacement was calculated according to Eq. (1).

$$1 - \frac{\text{EtBr displacement}_{\text{with alginate treatment}}}{\text{EtBr displacement}_{\text{without alginate treatment}}} \quad (1)$$

2.10. In vitro study of cell transfection

Human cell lines derived from liver (HepG2) and embryonic kidney (HEK-293T), as well as mouse fibroblasts (NIH/3T3) were obtained from American Type Culture Collection (Manassas, VA, USA). These cells were cultured in Dulbecco's modified Eagle's medium (DMEM, Gibco, Carlsbad, CA, USA) with 10% fetal bovine serum (FBS, Gibco).

Different N/P ratios of IL or SAP10 were used to complex with DNA and PEI in PBS as transfection reagents. Cells were seeded to 96-well multiplates (Corning, Lowell, MA, USA) one day before transfection. After removing medium, 50 μL of serum free DMEM and 50 μL of the transfection reagents were added per well. Normal culture medium (DMEM with 10% FBS) was replaced after 5 h incubation.

The activity of β-galactosidase was analyzed after 48 h of transfection to determine the expression efficiency of transgene. After removing culture medium, 40 μL of 0.25 M Tris-HCl was added and subsequent freeze/thaw cycles to lyze cells. Half of cell lysis reacted with ONPG for 30 min at 37 °C. The development was stopped by adding 62.5 μL of 1 M Na_2CO_3 and was quantified by the absorbance at 420 nm. These results were normalized by the protein amount of the other 20 μL of sample using BCA kit (Pierce, Rockford, IL, USA). The illustration of transfected cells was analyzed by X-gal staining. Briefly, 0.2% X-gal dissolved in DMF with 5 mM $K_4Fe(CN)_6$-$3H_2O$, 5 mM $K_3Fe(CN)_6$, and 2 mM $MgCl_2$ in PBS was prepared, and 100 μL was added for 37 °C staining overnight then rinsed with PBS. The staining images were illustrated using inverted microscope (Eclipse Ti−U, Nikon, Japan).

2.11. Viability of cell treated with peptides before and after DNA complexation

The effect of peptides and their complexation with DNA on cellular physiology was analyzed using 3-(4,5-dimethylthiazol-2-yl)-5-(3-carboxymethoxyphenyl)-2-(4-sulfophenyl)-2H-tetrazolium (MTS) assay. Peptides complexed with 0.5 μg DNA in different N/P ratios were incubated with NIH/3T3 cells. The same doses of peptides while without DNA incorporation were also applied to evaluate the effect of sole peptides on cell viability. After 48 h incubation, CellTiter 96 AQueous kit (Promega, Madison, WI, USA) was added 20 μL per well and

were incubated for 1 h at 37 °C, which were spectrophotometrically read at wavelength of 490 nm. These results were compared with the untreated cells for normalization and were expressed as cell viability.

2.12. Statistical analysis

SPSS (Chicago, IL, USA) was applied for statistical analyses, and a two-tailed Student's *t*-test was performed for comparison, in which the error bars were reported as standard deviations.

3. Results and discussion

3.1. Simulation to predict membrane perturbation of IL and SAP10 peptides

To predict the membrane association ability of modified SAP10 peptides, MD simulations were performed. Bilayers composed of POPC molecules were applied as simplified cell membranes, and the carbon-carbon order parameters of the lipid acyl chains, $<S_{CC}>$, were calculated to determine the levels of membrane perturbation upon IL and SAP10 association (Fig. 1a). Larger $<S_{CC}>$ meant more ordered acyl chains in the lipid bilayers. Compared to the untreated bilayer group, order parameters upon IL association were significantly decreased, suggesting that the acyl chains of the lipid bilayers were disturbed due to the existence of IL molecules. In contrast, the values of $<S_{CC}>$ as SAP10 association were slightly reduced, except for the tail of acyl chains (C10 to C18 at SN2 chain). The snapshots of these two peptides interactions with POPC lipid bilayers at simulation time of 80 ns were shown in Fig. 1b. For the IL peptides, a U-shape like structure embedded in the hydrophobic core (acyl chain of lipids). In particular, four aromatic residues (W4, W6, W8, and W9) inserted deeply into the hydrophobic cores of lipid bilayers. The POPC lipid head groups in upper leaflet were perturbed during IL association. In contrast, the snapshot illustrated that SAP10 anchored on the POPC lipid heads region with W3 and F5 insertion into the membrane hydrophobic core region.

From the analysis of MD simulations, we found that although IL and SAP10 were capable of disturbing lipid bilayers, the inserted IL and SAP10 peptides demonstrated different configurations. In this study, symmetric SAP10 (RRWKFFPWRR-$CONH_2$) peptides were modified from IL (ILPWKWPWWPWRR-$CONH_2$) by removing the hydrophobic domain (ILPWKWPW-) and replacing central –WW– to –FF–. Because hydrophobic tryptophan residues were extremely important to stabilize the inserted peptides in bilayer structures, especially W4, W6, W8, and W9, the reduction of tryptophan in SAP10 peptides led the inserted peptides only anchoring to the head heads of POPC. Similar results have been reported by Hsu et al. that their MD simulations demonstrated a boat-shaped conformation of IL in both phosphatidylglycerol and phosphatidylcholine lipid bilayers [32]. Because the cytotoxicity of IL has been reported to associate with tryptophan residues [17], the developed SAP10 peptides should reduce the effects of tryptophan on cell membranes. In addition, the snapshot and order parameters all indicated that hydrophilic SAP10 still could interact with lipid layers for membrane perturbation, suggesting this design was potential for delivery application

3.2. Validation of peptide effects on lipid structure

The MD simulations indicated that the developed SAP10 was potential to reduce membrane perturbation. Accordingly, we performed hemolysis experiments to evaluate the levels of membrane perturbation caused by peptides (Fig. 2a).[20] The complete hemolysis concentration of IL peptide was at 64 μM. In contrast with IL, SAP10 almost did not disrupt RBCs even at the highest concentration, suggesting that our designed SAP-10 peptide indeed reduced hemolysis and increase its applicability on drug delivery.

In order to investigate whether the low hemolysis of SAP10 was due to its low membrane perturbation, a SAXS experiments was applied. In this experiment, IL and SAP10 were examined for their influences on the mechanics, or more specifically on the spontaneous curvature, of a lipid monolayer formed by the zwitterionic lipid, DOPE. This lipid species was chosen both due to its abundance in cell membranes of eukaryotes [29] and its preference for forming the inverted hexagonal (HII) phase; formation of the HII phase is a prerequisite for measuring the variation in the spontaneous curvature or the spontaneous curvature *per se* of a lipid monolayer, as having been practiced routinely in many earlier studies [30,33–36]. Because dried DOPE was dispersed in the solution which had already contained the peptides, the peptides would automatically get into the water channels when DOPE self-assembled into the inverted structure. While the DOPE monolayer free of peptides displayed a negative spontaneous curvature (meaning that the surface of the monolayer would naturally bend toward the water side when the monolayer is free of any constraint), it is found that the spontaneous curvature became less negative (*i.e.*, the *magnitude* of the negative spontaneous curvature decreased) upon the addition to the samples of either IL or SAP10, with the latter having a more pronounced effect (Fig. 2b). In other words, the adsorption of IL or SAP10 to the DOPE monolayer and the following lipid-peptide interactions may have reduced the monolayer's tendency of bending toward the water side, even though the extent of the reduction was different between the two peptides.

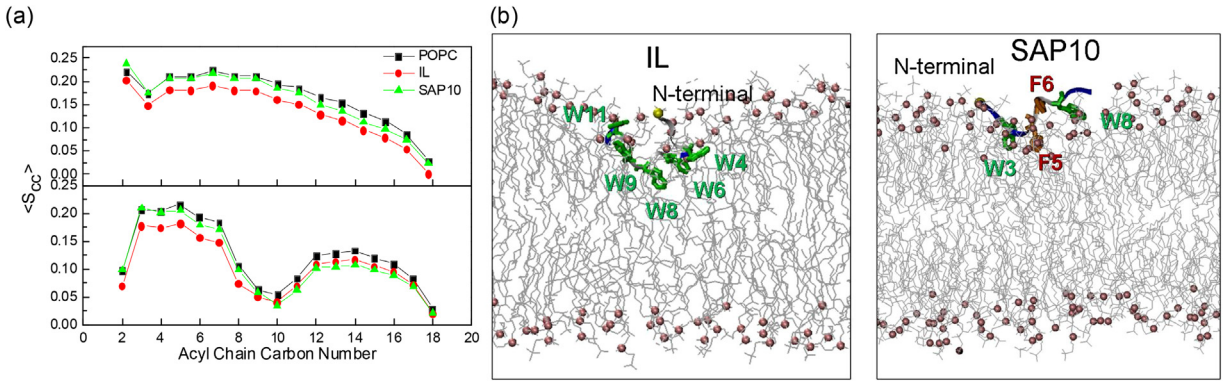

Fig. 1. Order parameter $<S_{cc}>$ and snapshots of the lipid acyl chains upon IL and SAP10 association.
(a) The carbon atoms are numbered sequentially from head to tail. The upper panel and lower panel are the $<S_{cc}>$ of POPC lipid's saturated (SN1) and unsaturated (SN2) aliphatic chains, respectively. The $<S_{cc}>$ of POPC lipid bilayes without peptide association was also calculated for comparison. (b) Snapshots at the 80 ns.

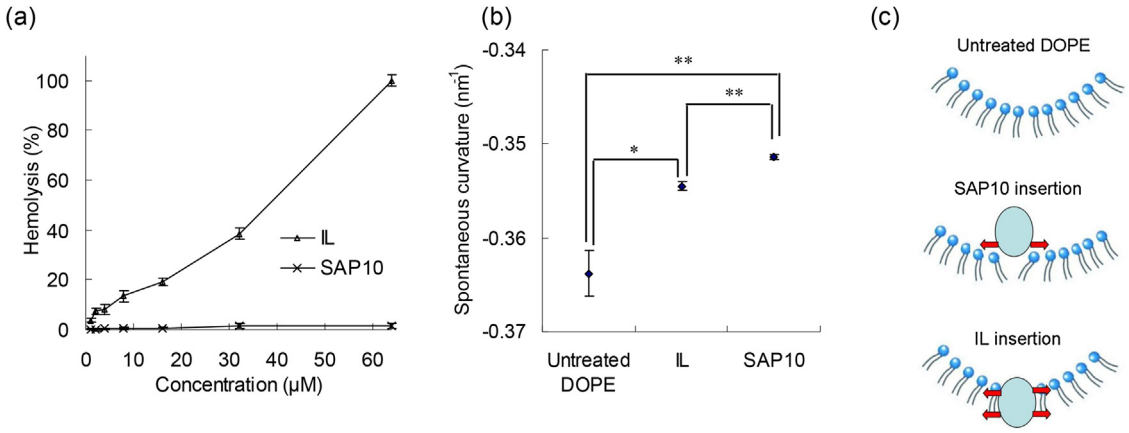

Fig. 2. Evaluation of membrane perturbation caused by peptides.
(a) The percentages of hemolysis caused by IL or SAP 10 at different concentrations. (b) The spontaneous curvatures of lipid monolayers formed by DOPE before and after IL or SAP10 treatments were determined with SAXS. (n = 3) (*t*-tests were applied for comparison. *: $p < .05$, **: $p < .01$) (c) The scheme of possible effect of peptide adsorption on the curvature of lipid monolayer.

The differential effects of IL and SAP10 on the spontaneous curvature may arise from the difference in the insertion depth into the monolayer of the two peptides. Indeed, it has been known from theoretical [37,38] and experimental [39] studies that the shallower a peptide is buried into a lipid monolayer, the stronger the tendency is for the surface of the monolayer to bend toward the *hydrophobic* side (*i.e.,* resulting in a preference for *positive* spontaneous curvatures). This phenomenon is correlated with how the peptide insertion affects the molecular shapes of the lipids: As the insertion is shallow, a peptide can effectively expand the molecular volumes in the headgroup regions of the lipids, leading to the monolayer's propensity of bending toward the hydrophobic side and exhibiting a positive spontaneous curvature. On the other hand, this preference for positive spontaneous curvatures gradually subsides and even turns to the inclination for negative spontaneous curvatures when a peptide penetrates deeper into the hydrophobic regions of the lipids and increases the molecular volumes therein (Fig. 2c).

Our spontaneous curvature measurements therefore indicate that IL was inserted more deeply into the DOPE monolayer than SAP10 and could consequently better maintain the preference for a negative spontaneous curvature of the DOPE monolayer than SAP10. This understanding is remarkably consistent with the results of our MD simulations, in which SAP10 was observed to reside in the headgroup regions while the insertion of IL had reached to the hydrophobic core of the POPC bilayer. Again, we argue that whereas both IL and SAP10 could readily interact with the lipid structures (which might be desired for the transfection facilitation), the discrepancy in the perturbation strength (or insertion depth) may ultimately differentiate the two peptide in terms of their cytotoxicity, which will be experimentally demonstrated in the following.

3.3. DLS analysis for complexed nanoparticles

Because negative-charged cellular membrane is the main barrier to the internalization of anionic DNA, an appropriate nonviral-vector should be able to decorate positive charges around DNA to promote gene delivery. In this study, we used peptides and PEI as carriers for DNA delivery. Compared to peptides, PEI has high density of positive charge, which may inhibit the complexation between peptide and DNA. Therefore, DNA was complexed with peptides before incorporating with PEI. Both zeta potentials and diameters of complexed nanoparticles were measured using DLS analysis (Fig. 3). Zeta potentials of DNA/peptide complexes increased with increasing N/P ratios analysis before PEI addition (Fig. 3a). It suggested that the electrostatic interaction may be a predominant determinant. Interestingly, the effect of SAP10 on increasing zeta potential was not as efficient as that of IL; the saturation of zeta potential of DNA/IL was at N/P 5, in contrast to that of DNA/SAP10 at N/P 40. We deduced that their differences probably were contributed by the charge densities of peptides. Because SAP10 has more positive amino acids in its sequence (R1, R2, K4, R9, and R10) than those of the IL (K5, R12, and R13), the numbers of SAP10 molecule were less than those of IL in equal N/P ratios. Sterically, more IL molecules may thus surround anionic

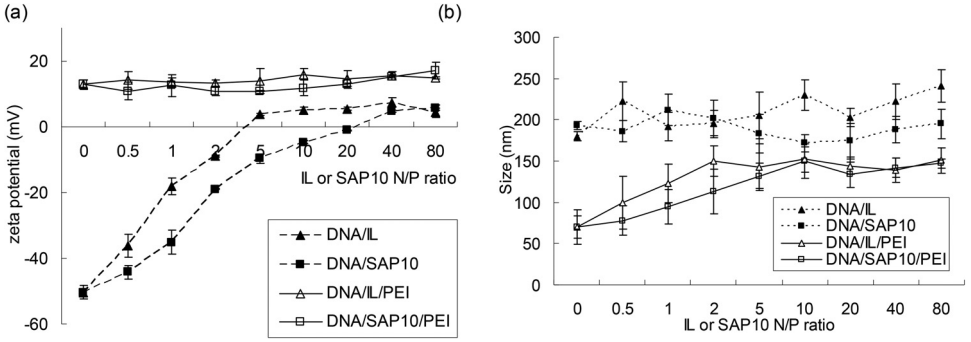

Fig. 3. Dynamic light scattering assay for determining the surface charge of complexed nanoparticles.
The (a) zeta potentials and (b) sizes of DNA/peptide and DNA/peptide/PEI complexes were analyzed in different N/P ratios of IL or SAP10 to DNA. For all groups, the N/P ratio of PEI to DNA was fixed to 10.

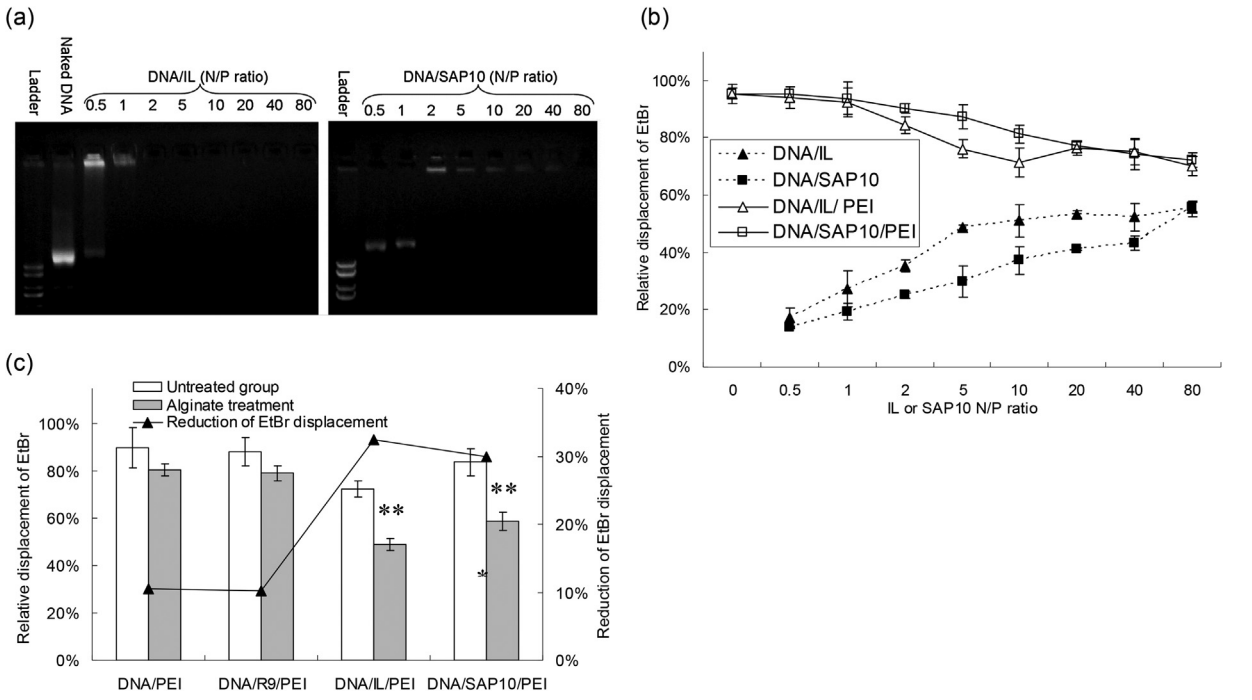

Fig. 4. The loading efficiencies and affinity of ternary DNA/peptide/PEI nanocomplexes.
(a) Different N/P ratios of DNA/IL and DNA/SAP10 complexes were applied to the gel retardation assay. The naked DNA was also performed as the control group. (b) The fluorescent dye exclusion assay. For the ternary nanoparticle groups, the N/P ratio of PEI to DNA was fixed to 10. (c) To determine the affinity between DNA and carrier molecules, anionic alginate was applied to compete with DNA and the EtBr displacement assay was performed to groups with or without alginate treatments. (*t*-tests compared the differences of the EtBr displacement results with and without alginate treatment. **: p < .01).

DNA more completely to lead to an efficient improvement on zeta potential. After PEI addition, all groups resulted in positive zeta potentials, suggesting that the formed ternary nanoparticles should equip appropriate surface charges for cell uptake.

For the size distribution, there was no significant trend of DNA/peptide nanocomplexes before complexing with PEI that all groups ranged between 180 and 240 nm (Fig. 3b). Pure DNA/PEI, *ie* the DNA/peptide/PEI groups at N/P 0, demonstrated high condensation ability that the formed particles reduced to 71 ± 13 nm. When IL or SAP peptides were applied for ternary nanocomplex preparation, these peptides slightly increased the sizes of nanocomplexes (Fig. 3b). Their sizes were saturated at ~150 nm and all groups were less than those of the corresponded DNA/peptide groups. Considering to the zeta potentials of ternary nanoparticles which did not change with the amounts of peptides (Fig. 3a), it suggested that the adsorbed positive charges from carrier molecules (PEI and peptides) seemed to be constant as the same amount of DNA was used for complexation. Therefore, the post-added PEI did not completely replace peptides, and thus DNA should complexed with both PEI and peptides.

3.4. Loading efficiency and dissociation ability of nanocomplex

Electrophoresis was applied to determine the efficiency of IL and SAP10 on DNA complexation (Fig. 4a). For IL, the leaked and smeared DNA band was found at N/P 0.5 and 1, respectively. There was no visible DNA in gel when N/P ratio was more than 1. For the SAP10 group, leaked DNA bands were also found at N/P 0.5 and 1. Although DNA was not leaked when the N/P ratios were further increased, the slight bands were observable below the wells, suggesting that the interaction between DNA/IL was tighter than that between DNA/SAP10.

The EtBr displacement assay was also performed for quantification (Fig. 4b). Similar to the gel retardation results, the DNA loading efficiency of IL was higher than that of SAP10. The saturation of DNA/IL appeared at N/P 5, compared to that of DNA/SAP10 at N/P 80. In contrast to peptides, PEI demonstrated superior complexation ability, whereas the complexation ability reduced with the increasing of peptides in ternary particles. Interestingly, the reduction effect of IL on ternary complex was more significant than that of SAP10. It may be due to that the interaction between IL and DNA was tighter than the corresponded SAP10 groups, which thus lessened the following PEI adsorption.

In additional to DNA encapsulation, an ideal gene carrier also needs to dissociate from DNA when they are internalized by host cells to ensure that the therapeutic genes can function without

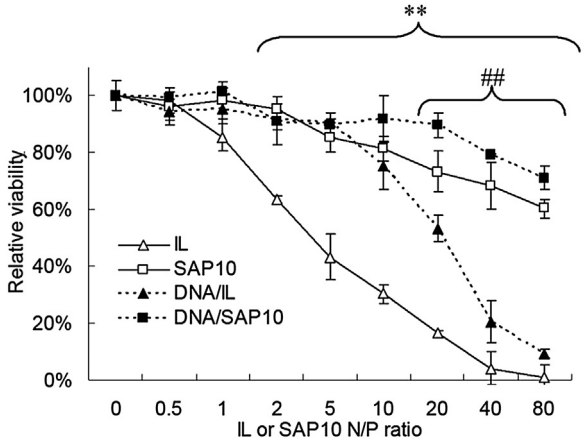

Fig. 5. Cytotoxicity of peptides and their complexation with DNA.
Sole peptides or peptides complexed with DNA were applied to treat NIH/3T3 cells for 2 days. The amounts of sole peptides were expressed as equal dose of peptide/DNA complex but without DNA incorporation. The MTS assay was performed, and the results were normalized by the untreated cell group. (*t*-tests were applied to compare the results of respective groups in the same N/P ratios. **: $p < .01$ for the results of the pure peptides; ##: $p < .01$ for the results of DMA/peptides groups).

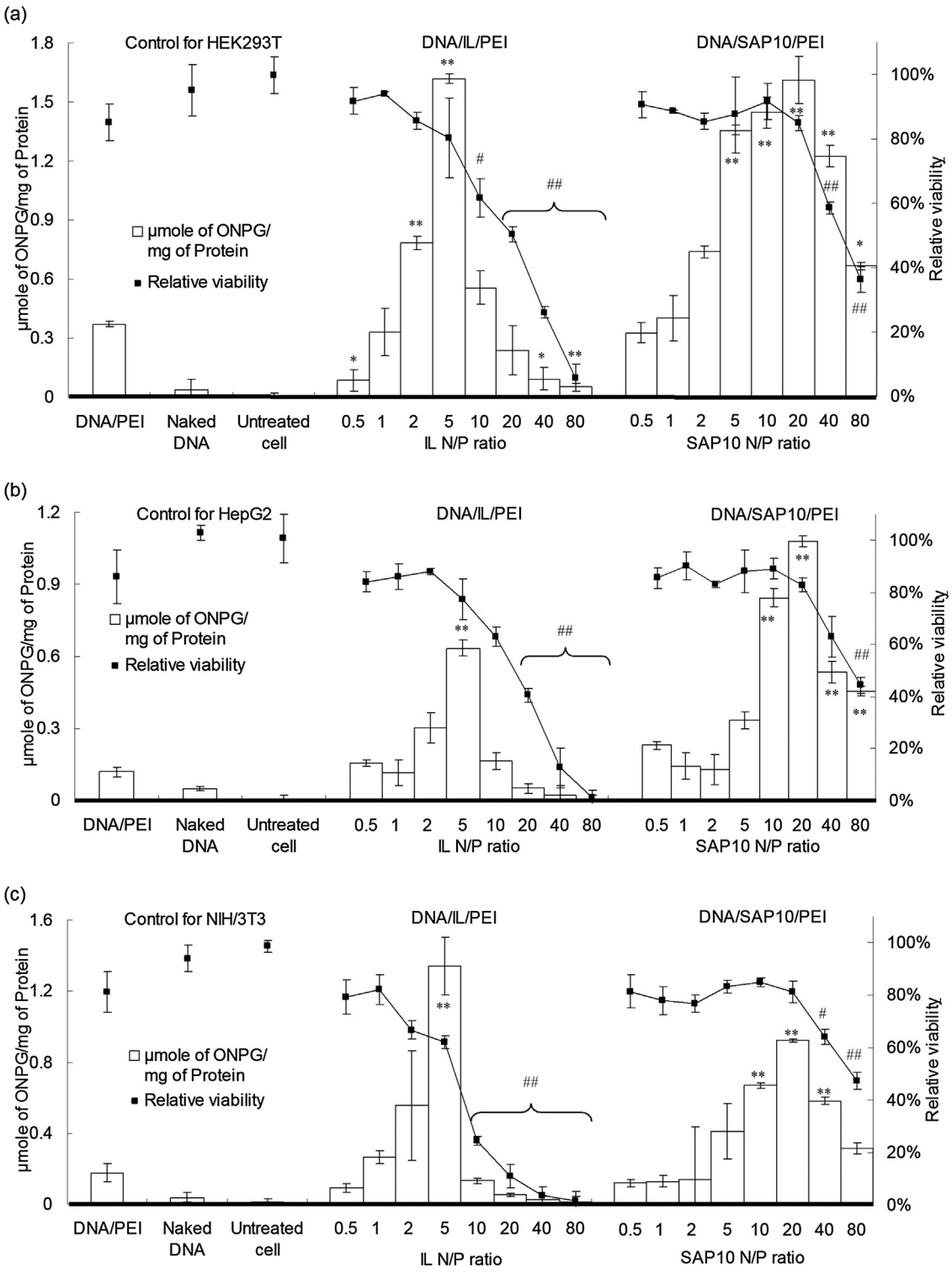

Fig. 6. in vitro transfection efficiencies of ternary nanoparticles.
Different N/P ratios of IL or SAP10 were applied to form ternary nanoparticles complexes with DNA and PEI for transfection to (a) HEK293T (b) HepG2 (c) NIH/3T3 cells. The N/P ratio of PEI to DNA was fixed to 10. The relative viability was also determined by MTS analysis. The PEI/DNA and the untreated cells were applied as the positive and negative control groups, respectively. (*t*-tests analyzed to the results of the DNA/PEI groups. *: $p < .05$, **: $p < .01$ for ONPG results; #: $p < .05$, ##: $p < .01$ for the MTS results).

interference from associated-carriers. To simulate the dissociation of DNA from carrier, a competition assay was applied that anionic alginate was added to destabilize complexed nanoparticles. Arginine-rich peptides are frequently used CPPs. Among them, nona-arginine (R9) was applied as the control group in this study because it has been identified as the optimal choice of the oligoarginine due to its high transduction frequency with low toxicity [40]. In addition, R9 should be a good control group to amphipathic IL because of its extremely hydrophilic property and high charge density [41]. The EtBr exclusion analysis was performed before and after alginate treatment, and the reduction of EtBr displacement after alginate treatment was compared to evaluate the interaction

between DNA and the carriers (Fig. 4c). By adding the same concentration of alginate, DNA/R9/PEI performed similar reduction ratio as that of DNA/PEI, suggesting that R9 did not alter the binding affinity so DNA can be stably complexed. In contrast, the addition of alginate demonstrated superior reduction for both IL and SAP10 involved ternary nanoparticles. These results indicated that the incorporation of IL and SAP10 weakened the interaction between DNA and PEI, and thus these internalized genes were capable of dissociating from carrier to execute their functions.

3.5. Cytotoxicity of peptides and their complexation with DNA

The major transportation mechanism of CPPs is correlative to their perturbation to cellular membrane [42]. Although CPPs have been broadly applied to transport different cargos, the membrane perturbation may elicit unwanted cytotoxicity [8,9]. Therefore, the cytotoxicity of sole peptides and peptide/DNA complexes were analyzed using MTS assay (Fig. 5). We first evaluated the toxicity of sole peptides. For convenient comparison with peptide/DNA results, the amounts of sole peptide groups were expressed as equivalent N/P ratios of peptide/DNA complexes but without DNA incorporation. Sole peptide demonstrated highly dose-depended cytotoxicity. Indolicidin significantly reduced cell viability which was less than 50% when the dose of IL was more than N/P 5. In contrast, SAP10 demonstrated only slight cytotoxicity that the cell viability can maintain more than 70% even when its application was more than N/P 80. These results suggested that the modified hydrophilic SAP10 was more biocompatible than IL. Furthermore, when these peptides were incorporated with DNA as complex, their cytotoxicities were greatly decreased.

Indolicidin peptide is an antimicrobial peptide which can against various pathogens because it may damage cell membranes due to electroporative disruption or toroidal pore formation [43–49]. Because IL is a tryptophan-rich peptide, it is extremely hydrophobic and may aggregate in aqueous environment, Subbalakshmi et al. have modified IL by replacing all tryptophan by phenylalanine [11]. Their results showed that the phenylalanine-modified IL peptides do not aggregate in aqueous solution and the hemolysis can thus be reduced. On the other hand, Yang et al. have designed the symmetric analogues of tritrpticin with amidation in C-terminal to preserve their antimicrobial activity whereas significantly reduce hemolysis activity [50]. Therefore, we combined these two concepts to design a SAP10 peptide. The SAP10 (RRWKFFPWRR-$CONH_2$) is a symmetric peptide derived from C-terminal of indolicidin (-WPWRR-$CONH_2$), and two central tryptophans were replaced by phenylalanines to reduce its steric hindrance in turn structure. Compared to IL, SAP10 has 6 cationic amino acids and there are only two tryptophan residues in the SAP10 sequence. Therefore, SAP10 is more hydrophilic and higher positive-charged than IL, suggesting the aggregation of SAP10 should be diminished in aqueous environment to reduce its cytotoxicity.

3.6. Transfection efficiency of peptides on different cells

For *in vitro* transfection experiments, ternary nanoparticles were prepared in different N/P ratios of peptides to DNA, in which DNA was always 0.5 μg and the PEI to DNA was maintained to N/P 10. Plasmid DNA encoding reporter *LacZ* gene was applied to quantify the transfection efficiency (Fig. 6). The results suggested that both IL and SAP10 significantly improved transfection compared to the PEI/DNA groups, which demonstrated peptide-dose dependent behaviors. The highest transfection efficiencies of DNA/IL/PEI and DNA/SAP10/PEI in different cells were always at N/P 5 and N/P 20, respectively. However, the transgene expression began declined as the N/P ratios of peptide kept growth, which was likely

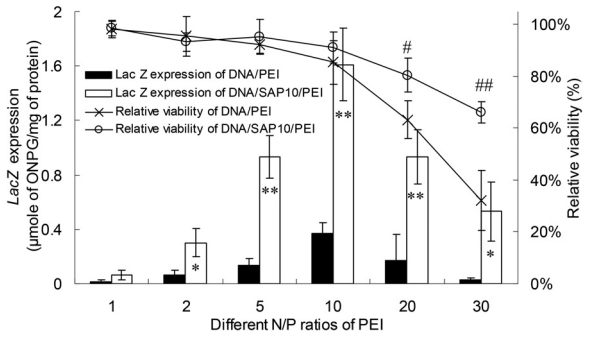

Fig. 7. The promotion effects of SAP10 on PEI-mediated gene delivery. SAP10 peptides were complexed with DNA in fixed N/P ratio of 20. Then, PEI was added in different N/P ratios to form ternary nanoparticles for gene delivery. (*t*-tests were applied to compare the corresponded results of DNA/PEI groups. *: $p < .05$, **: $p < .01$ for the ONPG results; #: $p < .05$, ##: $p < .01$ for the MTS results).

due to the cytotoxicity of peptides. Although both IL and SAP10 were capable of promoting PEI-mediated gene delivery, the high toxicity of IL restricted its application. Compared to IL which had narrow administration limit that N/P 2 had little function and N/P 10 induced high cytotoxicity, SAP10 can be safely used with appropriate transfection efficiency as the N/P ratios were between 5 and 40. Therefore, the broad administration window of modified SAP10 greatly reduced the risk and should be safe for gene delivery application.

In order to evaluate the effects of SAP10 on improving transfections efficiency, HEK293T cells were transfected using PEI-mediated gene delivery with or without SAP10 incorporation. In this experiment, PEI was applied in different N/P ratios but SAP10 was fixed to N/P 20 (Fig. 7). The transfection efficiency increased and then decreased with the N/P ratios of PEI in both formula, and the best results exhibited at N/P 10 of PEI. Among them, DNA/SAP10/PEI always demonstrated higher *LacZ* expression than those of the DNA/PEI groups. Gene delivery using sole PEI demonstrated a sharp decline as the N/P ratios were higher than 10, which should be resulted from the increasing of cytotoxic PEI. In contrast, cell viability of the DNA/SAP10/PEI groups was maintained even in the high N/P ratios. According to the EtBr displacement assay, the adsorption of PEI on DNA was competed by the firstly complexed SAP10 (Fig. 4b). By which, cell viability should thus be increased due to the reduction of internalized PEI. These results suggested that the incorporation of SAP10 not only promoted gene delivery but also decreased cytotoxicity of PEI-mediated gene delivery.

3.7. The effective peptides on PEI-mediated delivery are those complexed onto DNA

The transfection results demonstrated that IL and SAP10 can facilitate PEI-mediated gene delivery. During ternary nanoparticle preparation, the competition of PEI desorbed peptide from the complexes. It raised a question that the effective peptides on DNA delivery were those complexed onto DNA or those suspended in solutions as free form. To elucidate the mechanism, a three-step particles preparation was performed. First, DNA was complexed with IL or SAP10 at N/P ratio of 2. After PEI addition, free IL or SAP10 were supplied again to the transfection reagent so that the final N/P ratios of IL and SAP 10 were equal to 5 and 20, which were denoted as N/P $2 \rightarrow 5$ and N/P $2 \rightarrow 20$, respectively. The ONPG results demonstrated that the compensated peptides did not improved the gene delivery in both peptide groups (Fig. 8a). The tranfected cells were also stained by X-gal to illustrate transgene expression (Fig. 8b). Because our previous study indicated that the PEI owns higher charge density than those of the peptides, the complexed PEI inhibits peptides adsorption onto complexed

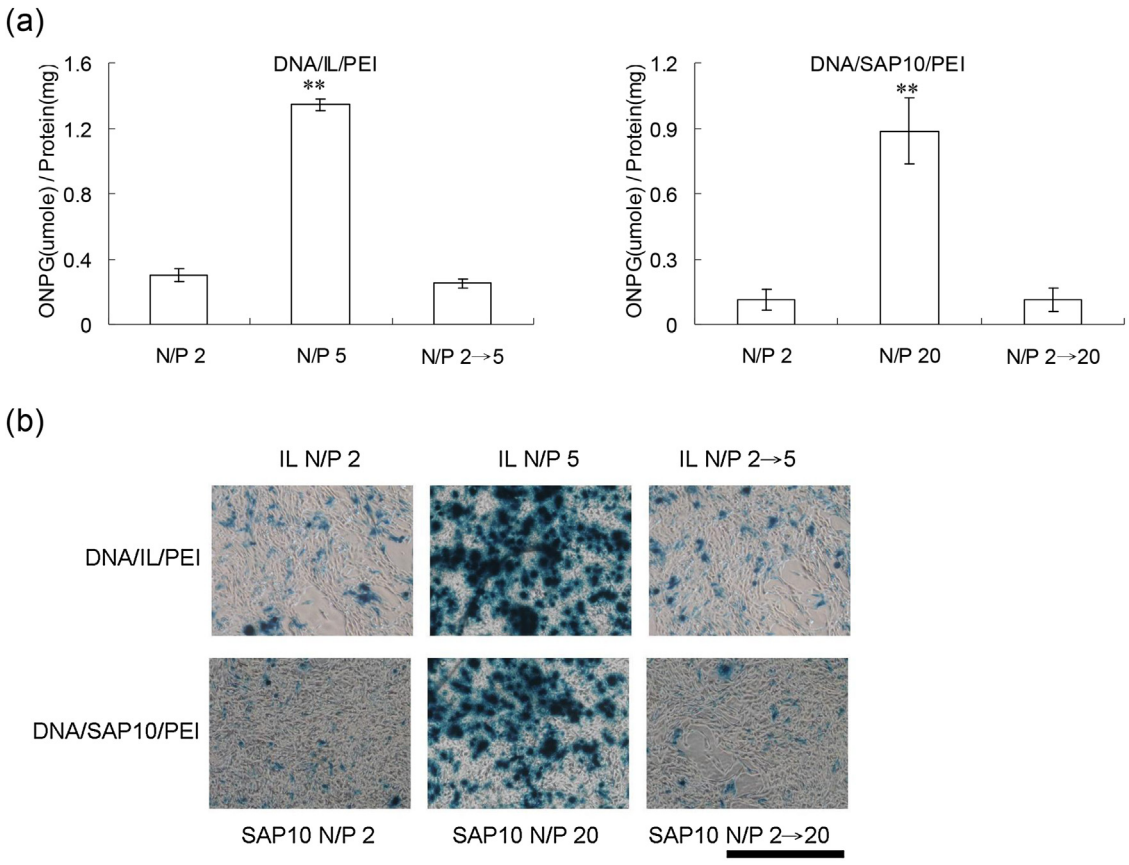

Fig. 8. The effects of compensated peptides on gene delivery.
NIH/3T3 cells were transfected by ternary nanoparticles prepared in different ways. (a) For the compensation groups, DNA was firstly complexed with IL or SAP10 at N/P ratios of 2. After PEI addition, free IL or SAP10 were supplied again to the transfection reagent so that the final N/P ratios of IL and SAP 10 were equal to 5 and 20, which were denoted as N/P 2 → 5 and N/P 2 → 20, respectively. (*t*-tests compared to the results of N/P 2. **: $p < .01$) (b) The transfected cells were stained by X-gal to illustrate transgene expression. (Scale bar = 500 μm).

nanoparticles [15]. Therefore, these extra-supplied peptides were unable to complex with DNA but suspended in solution as free-form. Combined these results, we concluded that only peptides adsorbed onto the complexed nanoparticles were capable of gene delivery facilitation.

4. Conclusions

SAP10, an almost mirror-symmetric peptide derived from IL is developed in this study. Both MD simulation and SAXS experiments indicate that the membrane perturbation of SAP10 is reduced compared to that of IL. Both IL and SAP10 enhance DNA dissociation from carriers, and they can be used as adjuvants to promote PEI-mediated gene delivery. Because SAP10 has high charge density and hydrophilicity, cells treated SAP10 demonstrate highly improved viability. The *in vitro* cell transfection results show that SAP10 preserves similar transfection efficiency as that of IL. Different from cytotoxic IL, the administration window of SAP10 can be broadened due to its high safety. The incorporation of SAP10 can also enhance the biocompatibility of PEI-mediated gene delivery. These properties ensure that SAP10 is potential as an efficient and safe carrier for gene delivery.

Acknowledgements

This research was supported by the grant of MOST 104-2221-E-008-105- from the Ministry of Science and Technology of Taiwan and 105 CGH-NCU-A2 from the National Central University and Cathay General Hospital Joint Research Center.

References

[1] G. Rassu, E. Soddu, A.M. Posadino, G. Pintus, B. Sarmento, P. Giunchedi, E. Gavini, Colloid Surf. B-Biointerfaces 152 (2017) 296–301.
[2] H. Jing, W. Cheng, S.Q. Li, B.L. Wu, X.P. Leng, S.P. Xu, J.W. Tian, Colloid Surf. B-Biointerfaces 146 (2016) 387–395.
[3] M. Lindberg, J. Jarvet, U. Langel, A. Graslund, Biochemistry 40 (2001) 3141–3149.
[4] D. Derossi, G. Chassaing, A. Prochiantz, Trends Cell Biol. 8 (1998) 84–87.
[5] J.B. Rothbard, T.C. Jessop, R.S. Lewis, B.A. Murray, P.A. Wender, J. Am. Chem. Soc. 126 (2004) 9506–9507.
[6] G. Tunnemann, R.M. Martin, S. Haupt, C. Patsch, F. Edenhofer, M.C. Cardoso, FASEB J. 20 (2006) 1775–1784.
[7] J. Bjorklund, H. Biverstahl, A. Graslund, L. Maler, P. Brzezinski, Biophys. J. 91 (2006) L29–L31.
[8] S. El-Andaloussi, P. Jarver, H.J. Johansson, U. Langel, Biochem. J. 407 (2007) 285–292.
[9] K. Saar, M. Lindgren, M. Hansen, E. Eiriksdottir, Y. Jiang, K. Rosenthal-Aizman, M. Sassian, U. Langel, Anal. Biochem. 345 (2005) 55–65.
[10] B. Behera, D. Mukherjee, T. Agarwal, J. Das, S.K. Ghosh, T.K. Maiti, Colloid Surf. B-Biointerfaces 140 (2016) 169–175.
[11] C. Subbalakshmi, V. Krishnakumari, R. Nagaraj, N. Sitaram, FEBS Lett. 395 (1996) 48–52.
[12] Y. Shai, Biopolymers 66 (2002) 236–248.
[13] C.W. Tsai, N.Y. Hsu, C.H. Wang, C.Y. Lu, Y. Chang, H.H.G. Tsai, R.C. Ruaan, J. Mol. Biol. 392 (2009) 837–854.
[14] T.I. Rokitskaya, N.I. Kolodkin, E.A. Kotova, Y.N. Antonenko, Biochim. Biophys. Acta-Biomembr. 1808 (2011) 91–97.
[15] W.W. Hu, Z.W. Lin, R.C. Ruaan, W.Y. Chen, S.L.C. Jin, Y. Chang, Int. J. Pharm. 456 (2013) 293–300.
[16] H.J. Schluesener, S. Radermacher, A. Melms, S. Jung, J. Neuroimmunol. 47 (1993) 199–202.
[17] C.W. Tsai, R.C. Ruaan, C.I. Liu, Langmuir 28 (2012) 10446–10452.

[18] M. Hallbrink, A. Floren, A. Elmquist, M. Pooga, T. Bartfai, U. Langel, Biochim. Biophys. Acta-Biomembr. 1515 (2011) 101–109.
[19] A.P. Podorieszach, H.E.K. Huttunen-Hennelly, Org. Biomol. Chem. 8 (2010) 1679–1687.
[20] B.L. Spaller, J.M. Trieu, P.F. Almeida, J. Membr. Biol. 246 (2013) 257–262.
[21] C.W. Tsai, W.W. Hu, C.I. Liu, R.C. Ruaan, B.C. Tsai, S.C. Jin, Y. Chang, W.Y. Chen, Int. J. Pharm. 494 (2015) 498–505.
[22] S. Jo, W. Im, Biophys. J. 100 (2011) 156.
[23] J.B. Klauda, R.M. Venable, J.A. Freites, J.W. O'Connor, D.J. Tobias, C. Mondragon-Ramirez, I. Vorobyov, A.D. MacKerell, R.W. Pastor, J. Phys. Chem. B 114 (2010) 7830–7843.
[24] A.D. MacKerell, M. Feig, C.L. Brooks, J. Am. Chem. Soc. 126 (2004) 698–699.
[25] W.L. Jorgensen, J. Chandrasekhar, J.D. Madura, R.W. Impey, M.L. Klein, J. Chem. Phys. 79 (1983) 926–935.
[26] L. Kale, R. Skeel, M. Bhandarkar, R. Brunner, A. Gursoy, N. Krawetz, J. Phillips, A. Shinozaki, K. Varadarajan, K. Schulten, J. Comp. Phys. 151 (1999) 283–312.
[27] P.J. Steinbach, B.R. Brooks, J. Comput. Chem. 15 (1994) 667–683.
[28] J.-P. Ryckaert, G. Ciccotti, H.J.C. Berendsen, J. Comp. Phys. 23 (1977) 327–341.
[29] G. van Meer, D.R. Voelker, G.W. Feigenson, Nat. Rev. Mol. Cell Biol. 9 (2008) 112–124.
[30] Y.F. Chen, K.Y. Tsang, W.F. Chang, Z.A. Fan, Soft Matter 11 (2015) 4041–4053.
[31] U.S. Jeng, C.H. Su, C.J. Su, K.F. Liao, W.T. Chuang, Y.H. Lai, J.W. Chang, Y.J. Chen, Y.S. Huang, M.T. Lee, K.L. Yu, J.M. Lin, D.G. Liu, C.F. Chang, C.Y. Liu, C.H. Chang, K.S. Liang, J. Appl. Crystallogr. 43 (2010) 110–121.
[32] J.C. Hsu, C.M. Yip, Biophys. J. 92 (2007) L100–102.
[33] D. Koller, K. Lohner, Biochim. Biophys. Acta-Biomembr. 1838 (2014) 2250–2259.
[34] B. Kollmitzer, P. Heftberger, M. Rappolt, G. Pabst, Soft Matter 9 (2013) 10877–10884.
[35] M. Chavarha, R.W. Loney, K. Kumar, S.B. Rananavare, S.B. Hall, Langmuir 28 (2012) 16596–16604.
[36] L.H. Yang, V.D. Gordon, D.R. Trinkle, N.W. Schmidt, M.A. Davis, C. DeVries, A. Som, J.E. Cronan, G.N. Tew, G.C.L. Wong, Proc. Natl. Acad. Sci. U. S. A. 105 (2008) 20595–20600.
[37] F. Campelo, H.T. McMahon, M.M. Kozlov, Biophys. J. 95 (2008) 2325–2339.
[38] A. Zemel, A. Ben-Shaul, S. May, J. Phys. Chem. B 112 (2008) 6988–6996.
[39] C. Galanth, F. Abbassi, O. Lequin, J. Ayala-Sanmartin, A. Ladram, P. Nicolas, M. Amiche, Biochemistry 48 (2009) 313–327.
[40] G. Tuunnemann, G. Ter-Avetisyan, R.M. Martin, M. Stoockl, A. Herrmann, C. Cardoso, J. Pept. Sci. 14 (2008) 469–476.
[41] Y.H. Dai, B.R. Liu, H.J. Chiang, H.J. Lee, Gene 489 (2011) 89–97.
[42] V. Teixeira, M.J. Feio, M. Bastos, Prog. Lipid Res. 51 (2012) 149–177.
[43] T.J. Falla, D.N. Karunaratne, R.E.W. Hancock, J. Biol. Chem. 271 (1996) 19298–19303.
[44] R. Halevy, A. Rozek, S. Kolusheva, R.E.W. Hancock, R. Jelinek, Peptides 24 (2003) 1753–1761.
[45] A.S. Ladokhin, M.E. Selsted, S.H. White, Biophys. J. 72 (1997) 794–805.
[46] D.G. Lee, H.K. Kim, S.A. Kim, Y. Park, S.C. Park, S.H. Jang, K.S. Hahm, Biochem. Biophys. Res. Commun. 305 (2003) 305–310.
[47] A. Rozek, C.L. Friedrich, R.E.W. Hancock, Biochemistry 39 (2000) 15765–15774.
[48] J.E. Shaw, J.R. Alattia, J.E. Verity, G.G. Prive, C.M. Yip, J. Struct. Biol. 154 (2006) 42–58.
[49] H.X. Zhao, J.P. Mattila, J.M. Holopainen, P.K.J. Kinnunen, Biophys. J. 81 (2001) 2979–2991.
[50] S.T. Yang, S.Y. Shin, K.S. Hahm, J. Il Kim, Int. J. Antimicrob. Agents 27 (2006) 325–330.